Thermal design of the CFRP support struts for the spatial framework of the Herschel Space Observatory

McDonald P.C.* Jaramillo E.** and B. Baudouy***

*Institute of Cryogenics, School of Engineering Sciences, University of Southampton, Southampton SO17 1BJ, UK
**HTS AG, Widenholzstrasse 1, CH-8304 Wallisellen, Switzerland
***Service des Accélérateurs, de Cryogénie et de Magnétisme, DSM/Dapnia, CEA/Saclay, 91191 Gif sur Yvette, France

Abstract
Thermal finite element (FE) models, of low thermal conductance struts which are required to provide support for the low temperature components of the Herschel Space Observatory, have been validated by measurements at temperatures below 20 K. The Herschel Space Observatory structure is introduced. FE modelling of two designs of support strut is briefly discussed and the final designs presented. Validation of the design models was made in two experiments. The first of these provided specific thermal conductivity data for component CFRP materials, whose composition was initially designed on the basis of data available in the literature. The second experiment was performed to confirm the thermal conductance (Q'/ΔT), of the completed struts. The validation test rigs are described together with details of the experimental methods employed. Values of conductance were at the level of $5 \cdot 10^{-5}$ W/K at a mean temperature of 6 K. The measured data are presented and discussed with reference to the thermal models. Sources of measurement inaccuracy, are also discussed.

Keywords: composites (A); heat transfer (C); thermal conductivity (C); space cryogenics (F)

1 Introduction

The Herschel Space Observatory is due for launch by the European Space Agency in 2007 and will capture images of the far infrared universe through three instruments:- a camera, a high resolution spectrometer and a photometer, all of which sit on an optical bench and are cooled to less than 3 K. The cooling of these instruments is to be achieved by placing the optical bench inside a large cryostat which contains a superfluid helium tank at 1.6 K and uses a circulation loop to deliver the superfluid helium to the bench. The configuration of the cryostat is illustrated by Figure 1, in which it may be seen that the optical bench and helium tank are supported from a "spatial framework" consisting of two aluminium frames which straddle the helium tank. The spatial frames are illustrated in Figure 2. The helium tank and optical bench are attached to the spatial framework by a system of axial and lateral struts and the frames are supported from the cryostat wall by an additional assembly of struts. The cryostat wall will be at an estimated temperature of 10 K.
This paper is concerned with the interface between the helium tank and the spatial framework. The interface has been designed to minimise heat transfer to the helium by using high strength low conductivity struts. The strut configurations are shown in Figure 3. They are constructed from carbon fibre reinforced plastic (CFRP) tube with crimped and glued aluminium alloy end fittings.
Following preliminary design modelling, thermal validation of the strut designs was made in two experiments. The first of these provided specific thermal conductivity data for component materials used in the modelling and the second measured the thermal performance of the completed struts. The designs of the validation test rigs are described together with details of the experimental methods employed.
In addition to providing adequate mechanical support with thermal isolation the interface structure must compensate for the thermal contraction of the tank, without inducing stresses on the optical bench and to this end the interface struts use MoS_2 coated ball and cup joints as end fittings, as shown in Figure 3 (b).

2 Strut design and thermal modelling

FE models were developed to predict heat transfer through the struts under varying temperature conditions, using thermal simulation software from MAYA [1]. The models included radiation heat

transfer from the cryostat wall. Initial modelling was done using thermo-physical property data obtained from [2] and [3]. Subsequently conductivity data for the CFRP was obtained by measurement as described in section 3 below, leading to the calculated values of conductance given in Table 1. Finally the strut models were validated by measurement of strut conductance as described in section 4. Table 1 shows values of conductance calculated from the FE model, for two different sets of boundary conditions. These are for:- cold end temperature: 1.6 K and cryostat wall temperatures of 6 K and 20 K. The predicted operating conditions are for a cold end temperature of 1.6 to 1.8 K and a high end temperature of 10 K, giving a mean temperature in the struts of approximately 6 K.
The CFRP tubes were constructed using T300 carbon fibre in an epoxy resin matrix (manufacturer reference: (Carbon Fibre FT300 6000-50B). The fibre content was 60% by volume, orientated at +/- 7° to the tube axis. The epoxy resin system was: Araldite XB3585 resin with XB 3403 hardener.

3 CFRP thermal conductivity measurements

Steady state measurements of the CFRP thermal conductivity were made by refrigerating one end of a sample at a constant temperature and then measuring the temperature gradient established across it when heat was applied to the free end. The experimental set-up, procedure and error sources are described below.

3.1 Experimental set up

The experimental set up is shown in Figure 4. It comprised an indium sealed vacuum can containing a copper cold stage upon which the CFRP sample was mounted. These were maintained at a constant temperature by immersion in a bath of superfluid liquid helium, whose saturated vapour pressure was controlled to within 0.13 mbar by means of a vacuum pump and PID control of a throttle valve.
The CFRP sample was attached to the cold stage by gluing it to a copper end cap, which was in turn glued to the cold head. To change samples, heat was applied to the copper cap to separate the two parts. The copper end cap was instrumented with a calibrated Germanium (Ge) temperature sensor to determine the cold end temperature, T_c, of the sample. A second copper cap was glued to the lower end of the sample and carried:- a heater (Constantan wire of 27 Ω) which was wired as a four terminal device, to produce heat (Q_m) required to establish a temperature gradient across the sample, and a second calibrated Ge temperature sensor, which was used to measure the hot end temperature, T_h, of the sample. To enable a calculation of heat loss from the sample due to thermal radiation, the temperature of the vacuum can wall was measured using a third Ge Sensor, glued to the inside wall with GE varnish.

3.2 Experimental procedure

The vacuum can was evacuated to 5 10^{-6} mbar at room temperature and liquid helium transferred into the cryostat. A small amount of helium exchange gas was then introduced in the vacuum can to accelerate the cool-down of the sample. When the sample reached 4.2 K, the exchange gas was evacuated and the liquid helium in the cryostat pumped to obtain the required base temperature. Heat, was then generated in the lower copper end cap and the temperatures monitored until a steady state was observed, at which point the heater current and voltage were measured. Repeated measurements were made with increasing sample hot end temperatures to produce the data shown in Figure 5.

3.3 Experimental errors

Principle sources of experimental error arose from:- errors in the measurement of temperature and heater powers and uncertainty in the heat flux through the samples due to heat transfer to and from the samples through extraneous sources. Errors in the measurement of sample dimensions were also considered.

3.3.1 Measurement errors

Errors in temperature measurement were estimated to be 10 mK over the test temperature range for the calibrated Ge sensors. The temperature sensor calibrations were verified by measurement of the vapour pressure in the saturated superfluid helium bath. Errors in the measurement of the heater power were minimized by four-terminal, voltage and current measurement and were better than 1% over the test temperature range. Measurements of the sample dimensions were made at room temperature and are shown in Table 2. Dimensions at low temperature were estimated from published data for the thermal

contraction of a T300 CFRP [4]. The thermal contraction of the composite in direction normal to the fibres is 0.95% from 300 K to 2 K and 0.93% from 300 K to 40 K. Whilst the contraction of the composite in direction parallel to fibres is 0.044% from 300 K to 2 K and 0.042% from 300 K to 40 K. Uncertainty in thermal contraction therefore is responsible for an error of less than 1% in the integral thermal conductivity calculation.
The samples were glued to the end caps over a length of 10 mm, using the epoxy resin "DP190" manufactured by the 3M Company. The thickness of the glue layer was estimated to be 0.1 mm. The conductivity of the glue, measured from 4 K to 10 K, was between 0.02 and 0.035 W/mK [5]. In our experimental configuration, the average thermal resistances created by the glue thickness were estimated to be 4.2 K/W and 3.4 K/W for the 25 and 31 mm diameter samples respectively, leading to errors in the measurement of sample temperature; T_h - T_c, of ~3 mK at 4 K and ~110 mK at 30 K. This corresponds to an accuracy of better than 0.5 %.

3.3.2 Heat flux uncertainty

Loss of heat from the sample due to molecular convection in the test cell was considered negligible, since the pressure of the vacuum can was maintained between 10^{-6} and 10^{-5} mbar during the test [6].
Heat losses by conduction Q_{pc} in the instrumentation wires and by radiation Q_{pr} from the sample and the copper block heater, were calculated and the results of these calculations were used to estimate a corrected heat flux Q_c through the sample from the measured heater power Q_m, by $Q_c=Q_m - Q_{pc} - Q_{pr}$. These calculations are estimations and were integrated into the error analysis; as a quadratic sum $\sigma_{Qc}^2 = \sigma_{Qi}^2 + \sigma_{Qpc}^2 + \sigma_{Qpr}^2$, with confidence factors of 20% for conduction and 50% for radiation.

3.3.3 Temperature sensor wire and heater wire conduction

Wire heat losses were calculated for each thermometer. The wires were made of Phosphor-Bronze (Ph-Br) and were 15 cm long with 0.2 mm diameter. They were connected to a feed-through (at the cold end temperature T_c) by copper wires (35 cm long and 0.2 mm diameter). To estimate the heat losses, the Ph-Br - copper wire junctions, were considered to be at an intermediate temperature, T_i. Heat flux was calculated using conductivity integrals for Ph-Br and copper (RRR=100) given in [4] and indicated T_i very close to T_c, meaning that there was no significant temperature gradient in the copper wires.
Estimation of the losses through the wires to the heater were based on the method described above, where the cross section of the copper wires was S_{cu}=1.96 10^{-7} m^2 (4 wires), and the length l_{cu}=3 m.

3.3.4 Sample and copper support radiation heat losses

Thermal radiation losses from the sample to the vacuum can wall, were estimated using T_m; the mean temperature of the sample between T_h and $T_{c,,}$ and T_{ref} the temperature of the vacuum can, which remained constant during the test. We assumed that the sample was primarily composed of T300 (carbon) and therefore had an emissivity close to 1 [7] and that there was no shape factor reducing the effective radiation heat transfer surface area ($S = \pi.D.h$ = 2.028 10^{-3} m^2).
Heat losses were only considered for the copper support cap holding the heater, at T_h, since the cold end support remained in thermal equilibrium with the vacuum can. We estimated the cap emissivity to be 0.1 [7] and again, that there was no shape factor reducing the radiation exchange surface area (S=1.88 10^{-3} m^2).

3.4 Conductivity calculations

Calculations were made using the measured data, to determine the thermal conductivity $\lambda(T)$ of the CFRP composite, as a function of temperature over the range of interest.

3.4.1 Determination principle

The Integral Method (THI method) was followed [8]. This method allows determination of the thermal conductivity without any constraints on the temperature difference or on the temperature variation of the thermal conductivity. For a steady-state, one dimensional heat flux, the integral of thermal conductivity (conductance) I, is given from the Fourier law by:-

$$I = Q\frac{l}{S} = \int_{Tc}^{Th} \lambda(T)dT \qquad (1)$$

where Q is the heat flux, S the area of cross section, l the distance between the cold and hot end temperature sensors T_c and T_h (copper end caps in our case). The measured variables were Q, l, S and the temperatures T_c and T_h. The thermal conductivity may be defined through:-

$$\frac{dI}{dT}(T_h) = \lambda(T_h) - \lambda(T_c)\frac{dT_c}{dT_h} \approx \lambda(T_h) \qquad (2)$$

If the temperature T_c is constant during the test, then the third term in (2) is negligible. One needs to introduce an analytical form for the integral and we propose to define the integral by a power series, then the thermal conductivity is expressed by:-

$$\lambda(T_h) = \sum_{i=1}^{n} a_n n \; T_h^{n-1} \qquad (3)$$

3.4.2 Experimental results and analysis

Figure 5 shows the variation of the measured temperatures with heater power, for the sample with 25 mm inner diameter. It may be seen that the T_c is almost constant over the entire power range.

Figure 6 shows the evolution of the thermal conductivity integral with increasing T_h for the same sample, where the data has been fitted by a power series. The order of the power series was optimized in order to obtain a χ^2coefficient close to unity and to minimise the errors in the a_i coefficients. The values of the optimised coefficients are shown in Table 3. Errors in the coefficients may be explained by the fact that they are strongly dependent on each other (dependency coefficient close to unity) which means that the associated error has to be seen as variation due to the error of the other coefficient. The error of the conductivity integral fit is given for a prediction interval of 1 σ (68%). The thermal conductivity is presented in Figure 7. Errors in the thermal conductivity are due to:- the integral measurement error, the propagation of this error through the fit and to the accuracy of the fit. It is found to be around 5%.

4 Model Validation measurements

Validation of the model was made by comparison with direct measurements of the conductances of sample struts, over the range 1.8 to 30 K.

4.1 Method

The method of measurement followed to determine the thermal conductances of the struts, was to:- mount one end of the selected samples of the struts on a surface cooled to 1.8 K, then apply heat to the free ends, observing their rise in temperature as functions of the heat supplied. The measurements were of very low conductances, measured at low temperatures and care was therefore taken in the design of the measurement system, to ensure that parasitic heat leaks were not significant in the measurements.

Measurements were made in a vacuum insulated cryostat, constructed as illustrated in Figure 8. Two samples of each strut design, were screwed to the base of a copper pot which could be filled with liquid helium at 4.2 K and then pumped; using a rotary vane vacuum pump, to reduce the vapour pressure of the helium to 16 mbar, thus obtaining a pot temperature of 1.8 K. The pot was suspended in the cryostat by two stainless steel fill/vent tubes which were used for the initial filling with liquid helium and subsequent pumping. A valve in the line to the pump was used to control the pumping speed and thus the helium vapour pressure. By this arrangement it was possible to control the helium temperature to 1.8 ± 0.1 K

An aluminium radiation shield was placed around the pot and was cooled by the first stage of a two stage G-M cryocooler, to approximately 50 K. The first stage of the cryocooler was also connected by a thermal link to the fill/vent tubes, to intercept conducted heat from ambient room temperature, which otherwise would have reached the pot. The second stage of the cryocooler was used to cool a charcoal sorption pump to approximately 10 K, to maintain a high vacuum in the cryostat and around the test samples. To minimise radiant heat transfer to the test sample, a second, aluminium radiation shield was screwed to the bottom of the helium pot and surrounded the samples. Ge resistance thermometers were attached to the bottom plates of the radiation shields and the shields were wrapped with multilayer super insulation.

4.2 Heaters

Heat was applied to the samples by means of electrical heater plates attached to the free ends of the struts. The heater plates used on the lateral struts were ~10mm thick aluminium disks, to which were glued 5×1 kΩ ceramic heater chips. The heater plates on the axial struts were constructed using ~5 mm thick copper

flanges to which were glued 10×1 kΩ ceramic heater chips. High heater resistances were selected so that the required operating current could be small and could be supplied using 0.127 mm diameter insulated phosphor bronze wires within the cryostat, without significant I^2R heating of the wires and without significant thermal conduction through them.
The heater plates were wired in series and therefore received a common current. Their relative resistance was chosen so that the warm end temperatures of the struts would be roughly the same during the tests and there would therefore be no heat transfer between them through the connecting wires.
The voltage across each heater was measured using pairs of non-current carrying voltage taps. These were made using the phosphor bronze wire and were thermally connected to the 1.8 K pot at a wire length of ~400 mm from the heaters. The thermal conductance of these, based on a material (Cu+5%Sn) conductivity of < 4 W/m.K [9] was calculated to be $1.3\ 10^{-7}$ W/K and conduction through the wires, from the heater at a temperature of 20 K, was conservatively estimated to be $2.4\ 10^{-6}$ W per wire. This represented <0.1% of the heater powers.

4.3 Thermometers

The aluminium ends of the struts were drilled and thermometers inserted. The thermometers used were Ge film on GaAs resistance thermometers, supplied by the Institute of Semiconductor Physics, Kiev [10]. They were individually calibrated over the range 1.8 to 300 K and supplied with individual interpolation polynomials and tables. Their R/T response was exponential with typical sensitivity at 1.8 K of ~-6.5 kΩ/K reducing to ~-23 Ω/K at 30 K. The thermometers were measured using a four-terminal arrangement of independent current (500nA) and voltage wires. As for the heaters, connection was made using phosphor bronze wires thermally anchored at 1.8 K and the conduction to the 1.8 K pot from each thermometer, for a warm end temperature of 20 K was therefore estimated to be $4\times2.4\ 10^{-6}$ W.

4.4 Data acquisition and conductance calculations

During measurement, thermometer resistances and heater powers, were logged at three minute intervals using an Agilent 34970A data acquisition unit. Temperatures were computed from the resistance values using thermometer specific R/T calibration curves. The increase in temperature, of the heated ends of the samples, were monitored until they reached a steady state, at which point the high and low end temperatures; T_h T_c were recorded together with the heater power. The heater power was then increased and the measurement process repeated, to produce a data table of the steady state temperatures versus heater powers. Conductance was calculated from the heater power divided by the steady state temperature difference observed across the samples (T_h-T_c), in units of W/K. The results are summarised in Figure 9 as curves of conductance versus T_h.

5 Results and conclusions

In conformance with the thermal conductivity analysis; (3.4.2), calculation of a fourth order polynomial fit to the conductance data shown in Figure 9, results in values of $1.04\text{x}10^{-4}$ and $3.1\text{x}10^{-5}$ W/K respectively, for the axial and lateral struts at the mean temperature of 6K, which is the expected mean operating temperature of the struts.
Table 4 compares the measured conductance data; (Figure 9), at high end temperatures of 6K and 20K to values predicted by FE modelling using the measured thermal conductivity data shown in Figure 7. The difference between the measured and modelled values is indicated as a percentage.
Differences between the modelled and measured results are very small in absolute terms and are not systematic. They are believed to arise from:- contact resistance, uncertainty in the effective dimensions of the insulating CFRP components of the struts; which employed glued and crimped aluminium end caps, and the long exponential approach to thermal equilibrium which takes place in the “low conductivity” materials, after a change in heater power. These issues could be addressed in future measurements but the data produced here was considered adequate for our present purposes.

References

[1] MAYA Heat Transfer Technologies Ltd., 4999 St. Catherine St. West, Suite 400, Montreal, Quebec, Canada H3Z 1T3. Thermal modelling was done using the TMG software package from MAYA

[2] Radcliffe, D.J: and Rosenberg H.M, The thermal Conductivity of Glass fibre and carbon fibre epoxy composites from 2 to 80 K, Cryogenics, p 245-249 May, 1982

[3] Bansemir, H and Haider,O, Basic material data and structural analysis of fibre components for space application, Cryogenics, vol. 31, p 298-306, Apr 1991

[4] Cryocomp 3.06, Cryodata Inc Florence SC, USA 29501

[5] F. Rondeaux, Ph. Brédy and J.M. Rey, Thermal Conductivity measurements of epoxy systems at low temperature, Advances in Cryogenic Engineering – materials, Vol. 48, p. 197-203, 2001

[6] G.K. White, Experimental techniques in low-temperature physics, Oxford University press, 1968

[7] Cryogénie et ses applications en supraconductivité, Institut International du Froid- Commission A1/2, Technique de l'Ingénieur, 1995

[8] J. Hust and A. Lankford, "Comments on the measurement of thermal conductivity and presentation of the thermal conductivity integral method," *Int. Journal. Thermophysic*, vol.3, pp. 67-77, 1982.

[9] Robert L. Powell and William A. Blanpied, Thermal Conductivity of Metals and Alloys at Low Temperatures, National Bureau of Standards Circular 556, September 1. 1954

[10] V.F. Mitin, Microsensor Ltd. http://www.microsensor.com.ua

Table 1. Predicted conductance data for axial and lateral struts with low end temperatures of 1.6 K and high end temperatures of 6 and 20 K.

High end temperature - K	**Conductance – $W.K^{-1}$**	
	Axial struts	**Lateral struts**
6	$8.4x10^{-5}$	$2.1x10^{-5}$
20	$2.7x10^{-4}$	$6.7x10^{-5}$

Table 2. CFRP sample dimensions at 300 K.

	Ø 25 mm	Ø 31 mm
Length (mm)	23.5 ± 0.1	23.5 ± 0.1
Thickness (mm)	3.00 ± 0.08	5.00 ± 0.07
Internal diameter (mm)	25.0 ± 0.4	31.0 ± 0.5

Table 3. Fitting Coefficients.

Coefficient	Value	Error
a0	-0.07032	0.03405
a1	0.03686	0.01937
a2	-0.00107	0.00293
a3	0.00009	0.00015
a4	-4.125410^{-7}	2.336510^{-6}

Table 4. Modelled and measured values of conductance for 6 K and 20K high end strut temperatures.

Strut	Temperature (K)	Model Conductance (W/K)	Measured Conductance (W/K)	Difference %
Axial	20	$2.7x10^{-4}$	$2.2x10^{-4}$	- 19
	6	$8.4x10^{-5}$	$6.6x10^{-5}$	-22
Lateral	20	$6.7x10^{-5}$	$7.9x10^{-5}$	+18
	6	$2.1x10^{-5}$	$1.0x10^{-5}$	-52

Figure 1. Schematic diagram of Herschel cryogenic assembly

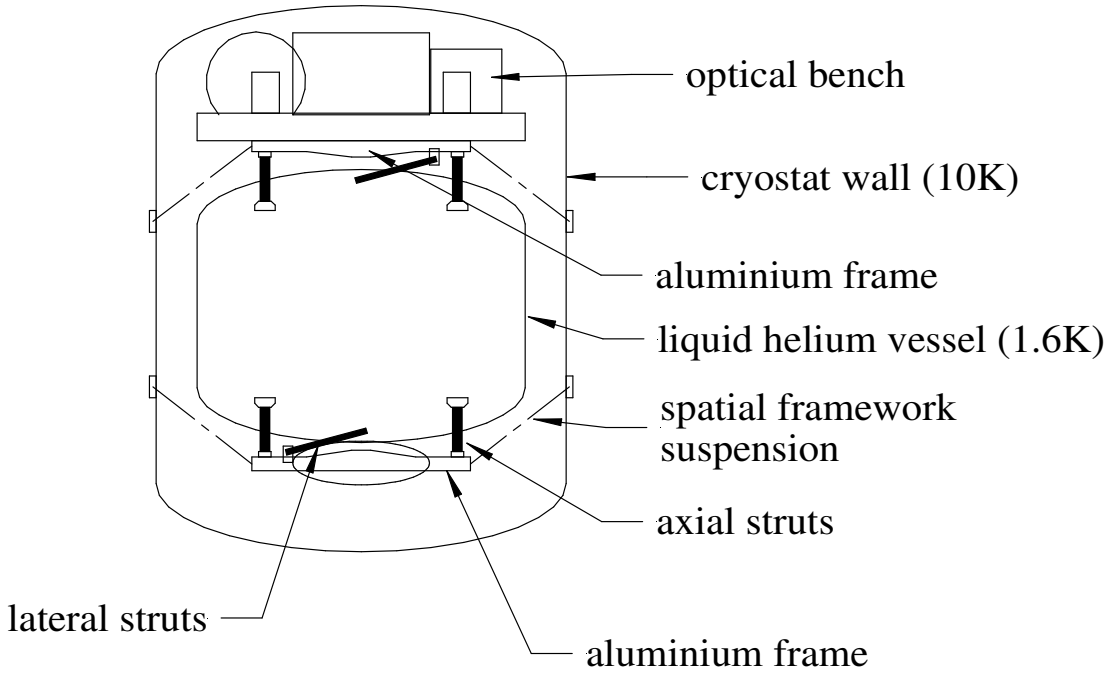

Figure 2. Lower spatial frame showing CFRP support strut.

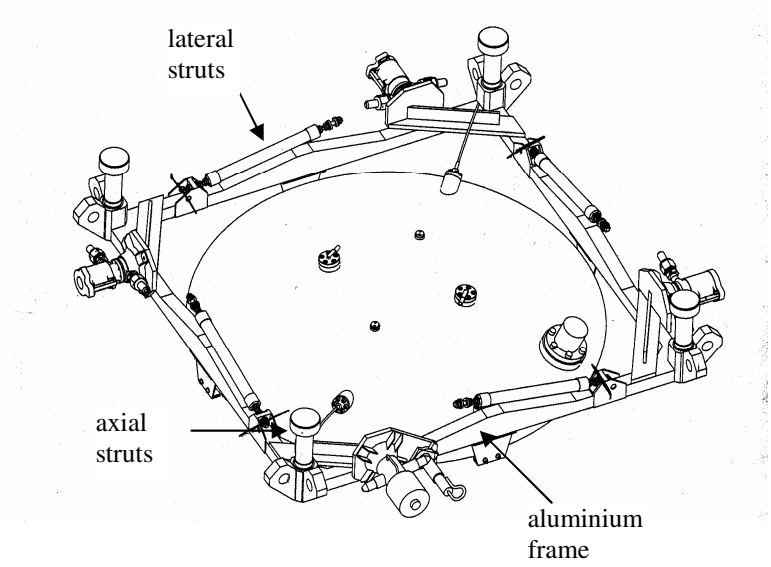

Figure 3. Lateral and axial struts

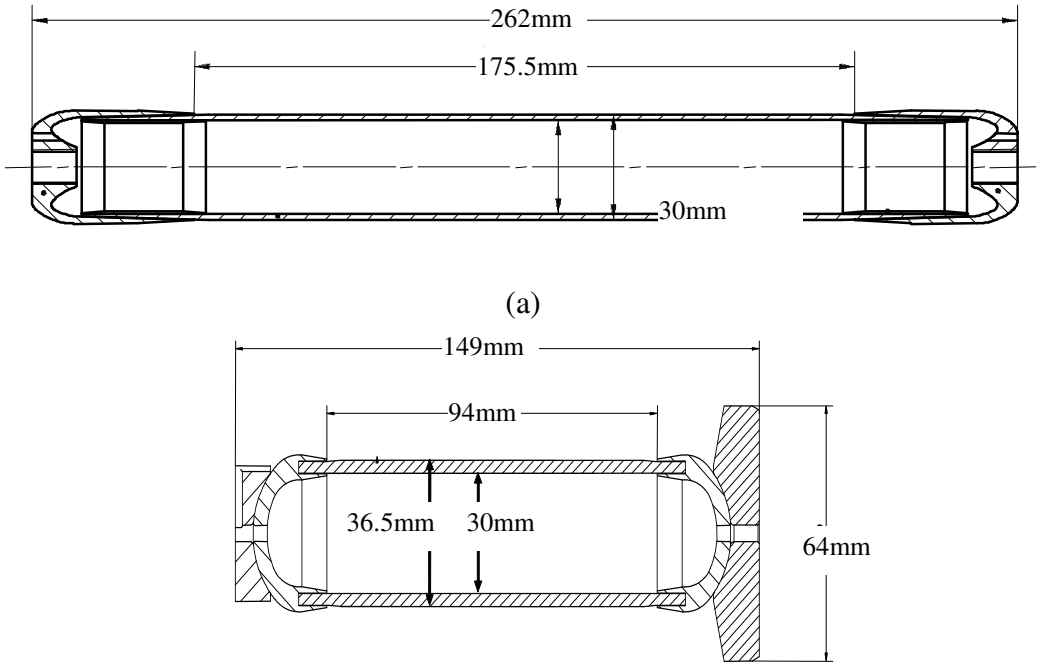

Figure 4 Thermal conductivity test cell

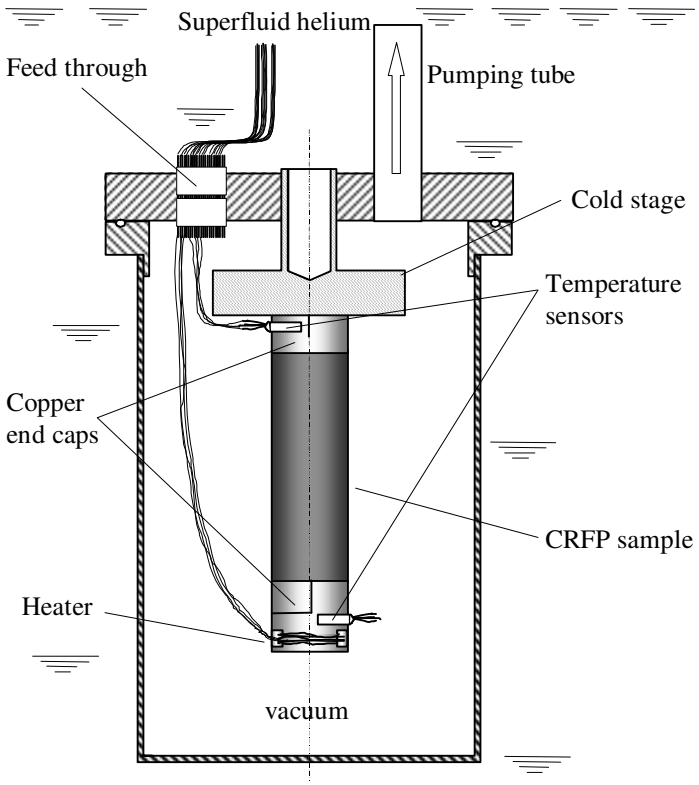

Figure 5. Evolution of temperatures T_c and T_h with Q_c for the Ø25 mm sample

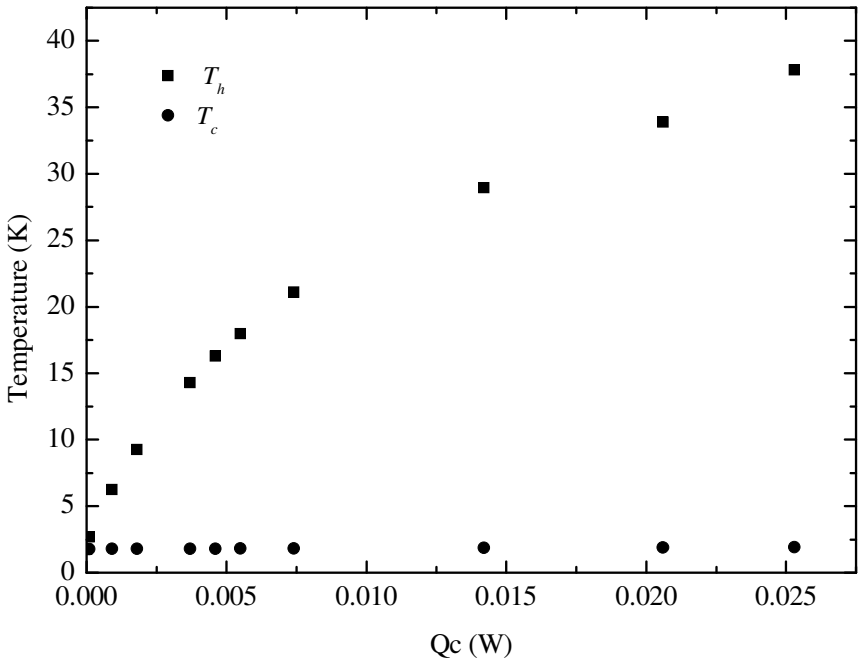

Figure 6. Evolution of conductivity integral as a function of T_h for the Ø25 mm sample

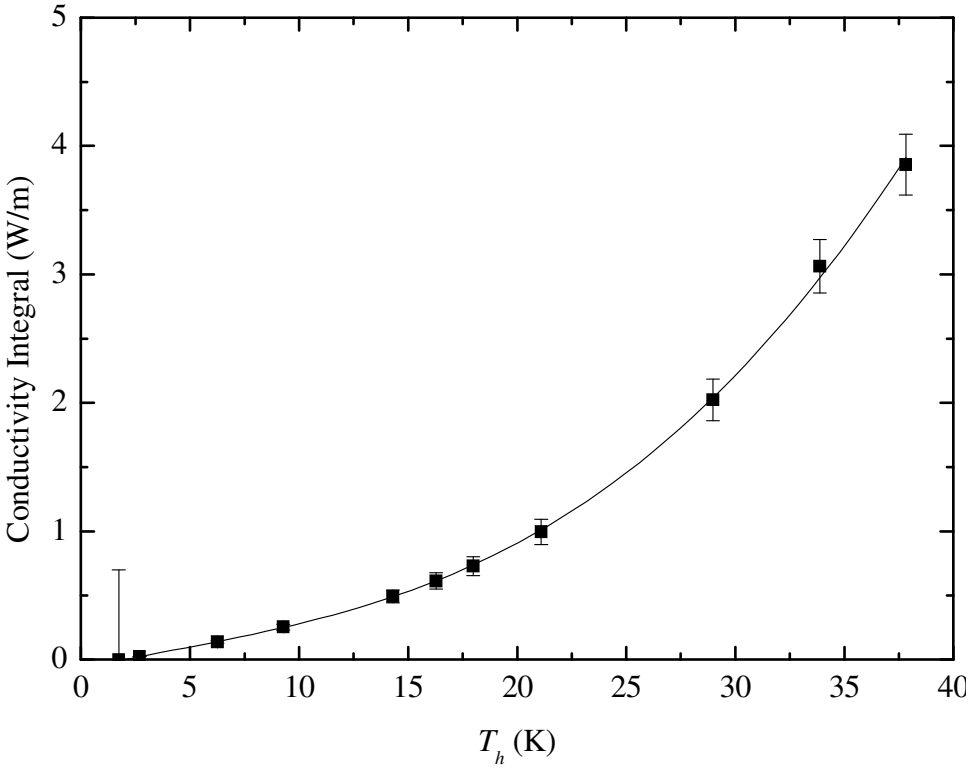

Figure 7. Evolution of the thermal conductivity with temperature

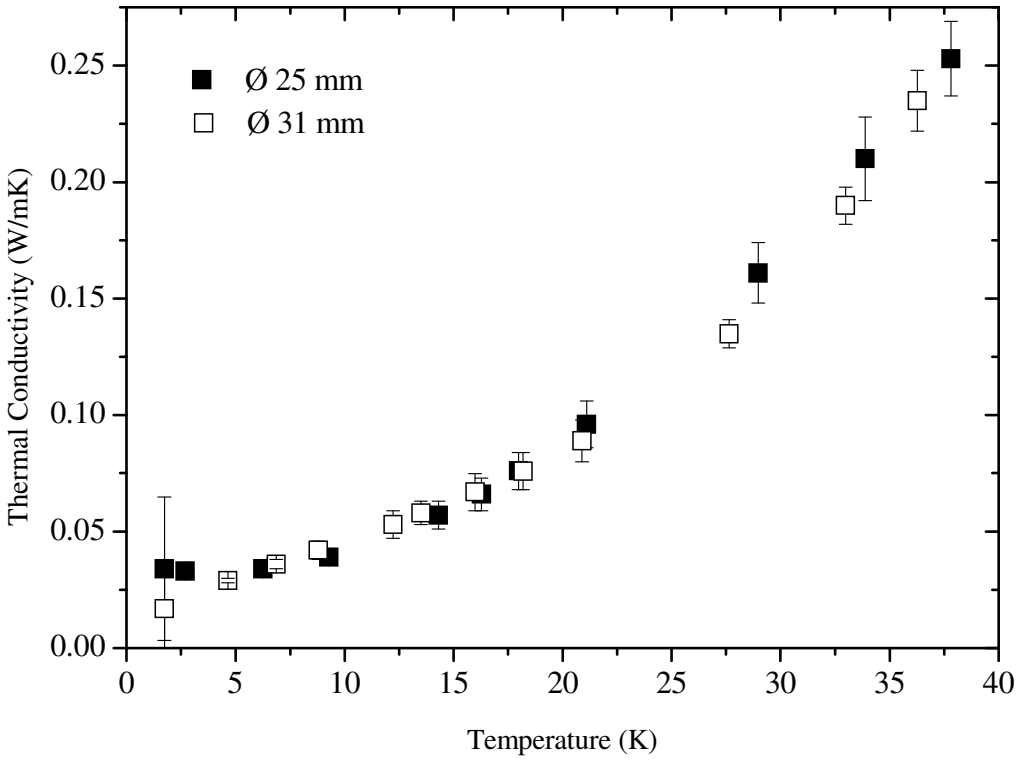

Figure 8. The test cryostat

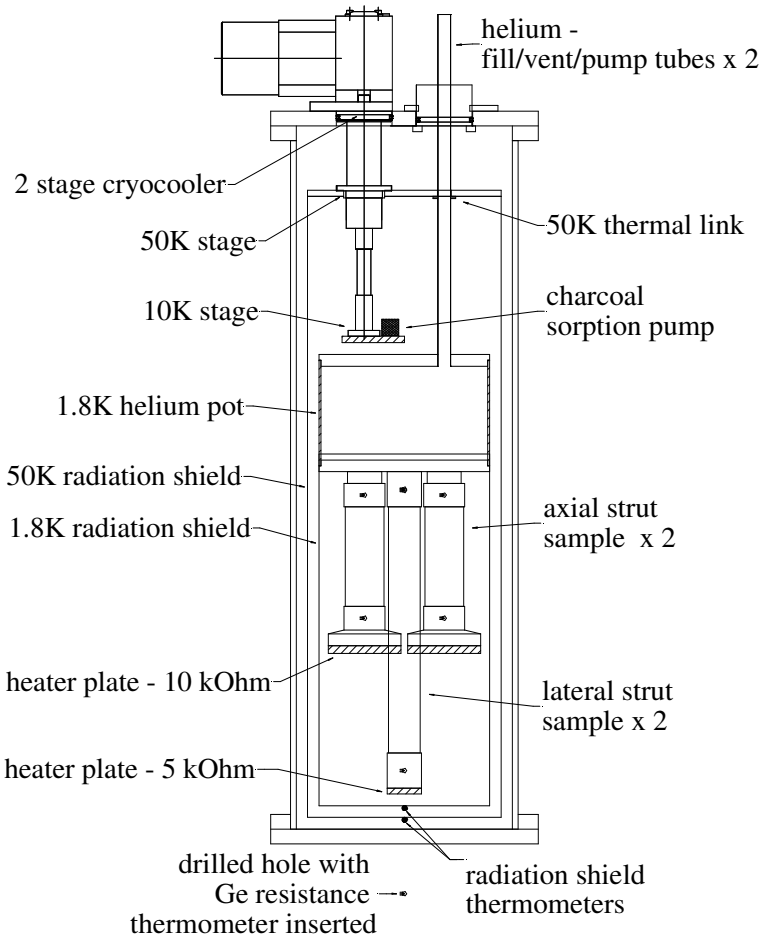

Figure 9. Measured conductance data